



## COVER SHEET

---

Clark, B.J. and Thambiratnam, David P. and Perera, N.J. (2006) Analytical and Experimental Investigation of the Behaviour of a Rollover Protective Structure. *The Structural Engineer*. **84(1):pp. 29-34.**

Accessed from <http://eprints.qut.edu.au>

Copyright 2007 Institution of Structural Engineers and (The authors)

# Analytical and Experimental Investigation of the Behaviour of a Rollover Protective Structure

B.J. Clark, D.P. Thambiratnam  
Queensland University of Technology, Brisbane, Queensland, Australia and  
N.J. Perera  
Managing Director, Bird & Marshal Ltd., U.K.

## Abstract

Rollover protective structures play a vital role in protecting the operators of large earthmoving machines which are commonly used in the rural and mining sectors. These structures typically consist of a moment resisting steel frame that is required to withstand the impact forces sustained by the vehicle during a rollover and provide a survival space for the operator during such an event. Recent advances in analytical modelling techniques have made it possible to model accurately the response behaviour of these types of structures when subjected to load and energy requirements according to current performance standards adopted both in Australia and internationally. This paper is concerned with the response behaviour of a rollover protective structure (ROPS) fitted to a 125 tonne rigid frame dump truck. Destructive experimental testing which involved the application of static loads to simulate the impact forces created during a rollover has been conducted on a ½ scale model ROPS for this particular vehicle. The testing program has involved complete instrumentation of the ROPS to enable corresponding member stresses and deflections to be recorded. In addition to this, non-linear finite element analysis has also been performed on this ROPS using the FEA software package ABAQUS version 6.3. The first stage of this computer analysis involved subjecting the ROPS to static loads about the lateral, vertical and longitudinal axes of the ROPS and comparing, results with those obtained from the experimental investigation and calibrating the computer model. Further research will involve using the calibrated finite element models to carry out dynamic simulations incorporating energy absorbing devices in the ROPS to optimize the level of energy absorption and enhance performance and operator safety.

## Introduction

Heavy vehicles which are commonly used in the rural and mining industries are particularly susceptible to rollovers as they commonly operate on sloping terrain and have a relatively high center of gravity. Rollover protective structures (ROPS) are fitted to these types of vehicles in order to protect the occupants by absorbing the energy of the impact created during the rollover. The design and analysis of these types of structures is complex and requires that a dual criterion be established that ensures that they are flexible enough to absorb energy, as well as being rigid enough to maintain a survival zone around the operator. Some research has been carried out on the behaviour of ROPS using analytical and experimental techniques (Clark et al, 2002; Kim et al, 2001; Tomas et al, 1997; Swan, 1988 and Hunckler et al, 1985)

The Dresser 630E dump truck is commonly used in the mining industry for the haulage of bulk material on site. This type of truck when fully loaded may carry up to 170t of material, which gives rise to a total gross vehicle weight of approximately 295t. In the event of a rollover, protection to the operator is provided through a combination of the ROPS positioned around the cabin and the vehicle's dump body. Figure 1 shows a typical Dresser 630E with the ROPS and dump body in place. Positioning of the ROPS is such that it encloses the cabin of the vehicle and permits a survival space for the operator during the event of a rollover. The survival space for the occupant is known as the DLV (dynamic limiting volume) and is a zone that is representative of a large seated male operator. For the ROPS design to be adequate, it must be capable of withstanding the load and energy requirements adopted by the relevant regulatory standard without intruding on the zone of the DLV. This paper presents the results of the experimental and analytical study that was conducted on a ½ scale model ROPS suitable for attachment to this particular vehicle,

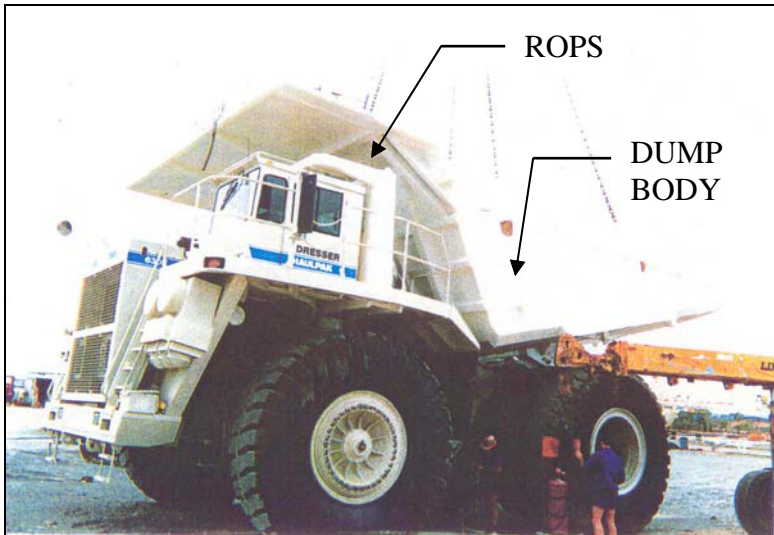


Figure 1 - Dresser 630E including ROPS and Dump Body

#### ROPS Description

The structural configuration of the Dresser 630E ROPS consisted primarily of a two post three dimensional moment resisting frame that cantilevered directly from a tapering box beam that was fixed directly to the chassis of the vehicle. All impact loads sustained by the ROPS during a rollover are transferred through this beam directly into the chassis of the vehicle. Member types employed for this structure consisted of 350 grade steel rectangular/square hollow sections (RHS/SHS) with fully welded moment resisting connections. Haunches fabricated from the same RHS/SHS material were employed to strengthen zones that would be highly stressed during loading. Figure 2 shows an illustration of the  $\frac{1}{2}$  scale model ROPS that was tested in the structures laboratory of the Queensland University of Technology. Also shown in this figure is the method in which the ROPS is typically connected to the chassis of the vehicle.

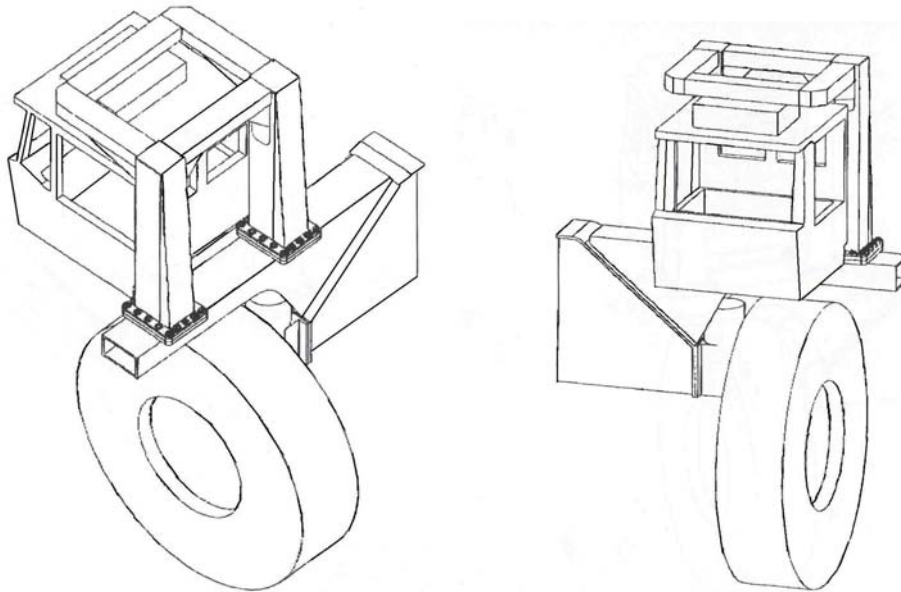


Figure 2 – ½ scale ROPS and ROPS attachment to Dresser 630E

### Similitude Modelling

Previous research conducted by Srivastava et al (1978) had shown that the principles of similitude modelling could be successfully applied to ROPS testing techniques. The authors had highlighted that the use of such principles could lead to large scale economic savings when conducting tests on ROPS. Based on the research findings of these authors the principles of similitude were applied to the Dresser 630E ROPS in order to lessen fabrication costs and reduce the magnitude of the loads that were required to be applied to the ROPS during testing. Reduction in the magnitude of the loads was essential as a full scale test of a ROPS for a vehicle such as this were extremely large and would require the use of an extensive laboratory testing facility.

Buckingham's pi theorem was employed to determine the number of independent dimensionless parameters that would influence the behaviour of the system. Once the independent pi terms were determined, they were equated between the model and prototype ROPS to establish the model design conditions. A scaling factor of ½ was then selected between the model and prototype which gave rise to the following relationships which are shown in table 1.

Table 1 – Relationship between model and prototype parameters

$(I_{xx})_m = \left(\frac{I_{xx}}{16}\right)p$	$(I_{yy})_m = \left(\frac{I_{yy}}{16}\right)p$	$(U_{Lateral})_m = \left(\frac{U_{Lateral}}{8}\right)p$
$(F_{Lateral})_m = \left(\frac{F_{Lateral}}{4}\right)p$	$(F_{Vertical})_m = \left(\frac{F_{Vertical}}{4}\right)p$	$(F_{Longitudinal})_m = \left(\frac{F_{Longitudinal}}{4}\right)p$
$(\Delta_x)_m = \left(\frac{\Delta_x}{2}\right)p$	$(\Delta_y)_m = \left(\frac{\Delta_y}{2}\right)p$	$(\Delta_z)_m = \left(\frac{\Delta_z}{2}\right)p$

Where:

- $I_{xx}$ : Second moment of area of the ROPS structural members about the x axis
- $I_{yy}$ : Second moment of area of the ROPS structural members about the y axis
- $U_{Lateral}$ : Lateral energy absorption requirement for the ROPS
- $F_{Lateral}$ : Lateral load requirement for the ROPS
- $F_{Vertical}$ : Vertical load requirement for the ROPS
- $F_{Longitudinal}$ : Longitudinal load requirement for the ROPS
- $\Delta_x$ : Deflection of the ROPS in the lateral direction
- $\Delta_y$ : Deflection of the ROPS in the vertical direction
- $\Delta_z$ : Deflection of the ROPS in the longitudinal direction

and the subscripts m and p represent the model and prototype respectively

### Experimental Investigation

Using the relationships derived from the similitude analysis, a half scale ROPS was fabricated and tested in accordance with the laboratory testing procedure outlined in (AS2294.2-1997). These testing methods simulate impact loads created during a vehicle overturn through the application of static loads about the lateral, vertical and longitudinal axes of the ROPS. The standard also requires that a predefined amount of energy must be absorbed by the ROPS in the lateral direction. Figure 3 shows an illustration of the ROPS indicating how the static loads are applied in accordance with the Australian standard. In addition to this the member sizes used for the test model ROPS have also been shown in Table 1.

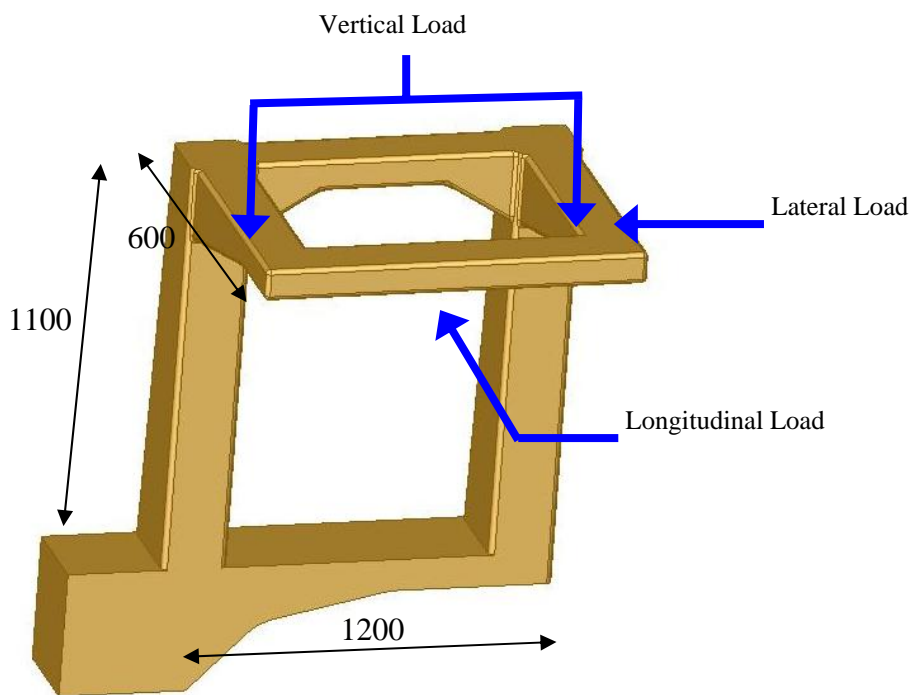


Figure 3 – ROPS Load application

**Table 1 ROPS Member Sizes**

ROPS Member	Member Type
Posts	350 grade 150x150x6 RHS
Front Cross Beam	350 grade 125x75x5 RHS
Rear Cross Beam	350 grade 125x75x5 RHS

Side Beams	350 grade 125x75x5 RHS
Haunches	350 grade 125x125x5 SHS
Internal Stiffener plates	350 grade 6mm plate
Chassis Beam	350 grade 16mm plate

The magnitudes of these loads and the energy absorption requirement are primarily derived from information relating to the type of vehicle to be tested and its mass. For rigid frame dumpers such as the 630E, the standard allows the peak loads about the lateral and longitudinal directions as well as the energy absorption in the lateral direction to be reduced by 40% to allow for sharing of the impact loads between the ROPS and the vehicle's dump body. A summary of the loads that were applied to the half scale ROPS taking this 40% reduction into account and based on a full size vehicle mass of 100168 kg, are presented in table 2.

Table 2 - AS2294.2 Loads:

Item	AS2294.2 Requirement with scaling provision allowed	Result for ½ scale model
$F_{\text{Lateral}}$ : (Lateral Force)	$\left(\frac{1}{4}\right) \cdot 0.6 \cdot \left[ 413500 \left(\frac{M}{10000}\right)^{0.2} \right]$	98000 N
$U_{\text{Lateral}}$ : (Lateral Energy Absorption)	$0.6 \cdot \left[ 61450 \left(\frac{M}{10000}\right)^{0.32} \right]$	9634 J
$F_{\text{Vertical}}$ : (Vertical Force)	$\frac{1}{4} \cdot 19.61M$	491000 N
$F_{\text{Longitudinal}}$ : (Longitudinal Force)	$\frac{1}{4} \cdot 0.6 \cdot \left[ 330800 \left(\frac{M}{10000}\right)^{0.2} \right]$	79000 N

Description of test setup

The ROPS and associated tapering box beam were mounted to a specially fabricated loading frame that could safely apply the required lateral, vertical and longitudinal loads. Attachment of the ROPS to the loading frame was performed through a stiff bolted moment resisting connection at the base of the box beam. This connection which is shown in figure 4 was designed to simulate the true connection of the box beam to the chassis of the 630E dump truck. The loading frame that was assembled at QUT's structures laboratory is also shown in figure 4.



Figure 4 – Testing framing and ROPS connection

Instrumentation and measurement parameters

Strain and deflection measurements were taken during each loading sequence through the use of an Agilent Technologies’ 120 channel VXI data acquisition system. 8 Strain rosettes with 5mm gauge lengths were strategically positioned throughout the structure in regions of predicted high levels of strain and recordings were taken at consistent intervals during each loading sequence. After each loading stage, the strain rosettes that measured strains beyond yield were replaced. Deflection of the ROPS was measured using LVDT’s that were placed at four locations within the structure. The LVDT’s were securely mounted to an independent steel frame that enabled true readings to be taken about each axis of the ROPS. Polished stainless steel plates were attached to the ROPS at the location of each LVDT, to enable the ROPS to slide independently of each deflection monitoring device. The use of these plates was particularly important as the ROPS underwent significant deflection about all three axes during each loading stage. Load generation for each stage was performed using hydraulic jacks that were powered by an electric pump. These jacks were calibrated prior to testing to enable accurate load measurements to be recorded by the data acquisition system during testing. Figure 5 presents an illustration of the ROPS showing the positions of the strain rosettes and the LVDT’s.

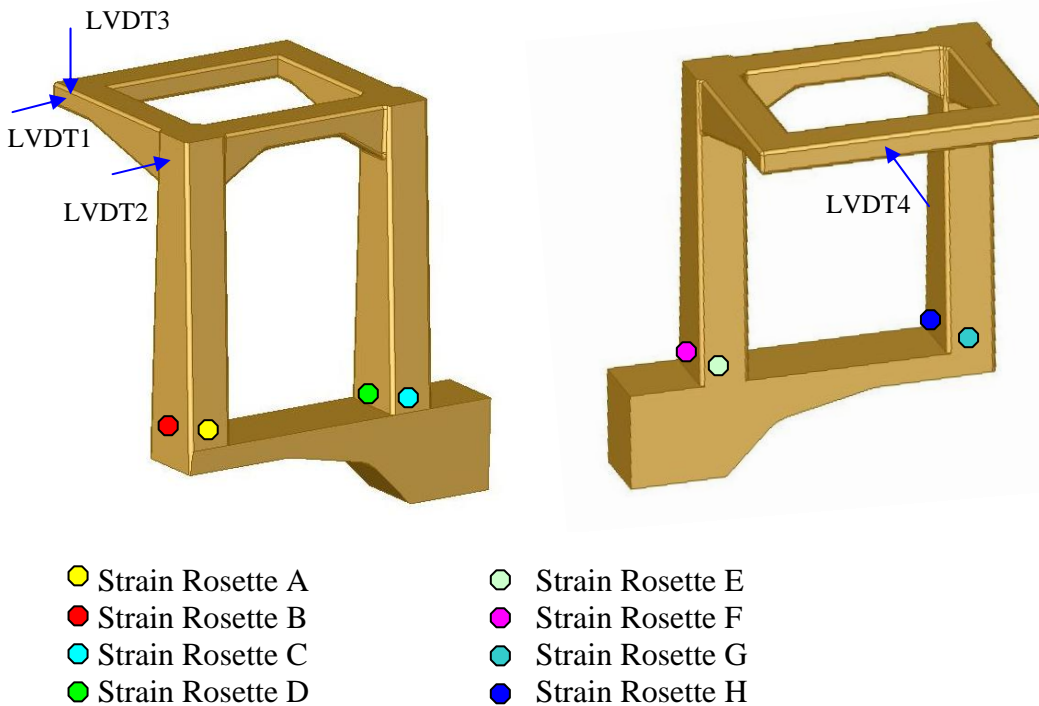


Figure – 5 LVDT and Strain rosette positions

Lateral loading phase

Lateral loading of the ROPS was conducted using a 50 tonne Enerpac hydraulic jack that was mounted to the horizontal loading beam of the testing frame. The load was positioned 235mm from the inside face of the left side ROPS post which corresponded to the vertical projection of the DLV, as required by AS2294 (1997). Load spreading to prevent localized deformation was achieved by using a unique system that consisted of two 50mm thick steel reinforced bridge bearings that were sandwiched between two 25mm thick steel plates.

The load spreading system was devised as a result of the expected deflection of the ROPS about each axis during application of the lateral load. The layout of the ROPS and connection to the loading frame, indicated that it would move significantly forward, upward and sideward during application of the lateral load. Concern was raised over the expected eccentric loading of the hydraulic jack and its probable damage during this loading sequence. The incorporation of the bridge bearing system meant that localized shear deformation of each bearing could take place with very little axial squashing of the bearing itself. This shear deformation which was within the allowable limits of the bearings, was used in conjunction with a steel ball and seat at the end of the jack. This arrangement allowed

the jack to remain predominantly in its original position when applying the lateral load and thus prevented any damage to the jack.

The lateral load was applied gradually in order to simulate static conditions and both strains and displacements were recorded at regular intervals until the code specified minimum lateral load was achieved. Examination of the resulting load deflection profile at this level of loading, which is shown in figure 7, indicated that the ROPS had not absorbed enough energy to fulfill the requirements of the standard. A substantial increase in both the lateral load and the lateral deflection of the structure was required in order to achieve this energy level. Loading was subsequently continued until the area under the load deflection curve equated approximately to the code specified value. This requirement was achieved at a lateral load of 325 kN and a corresponding lateral deflection of 53 mm. Once the energy requirement was achieved, the ROPS was unloaded with a resulting permanent deflection of 13mm in the lateral direction. The deflected shape of the ROPS under lateral load, load deflection profile for the ROPS in the lateral direction and load deflection profiles about all three axes during this loading stage are shown in figures 6, 7 and 8 respectively.



Figure 6 – ROPS under lateral load

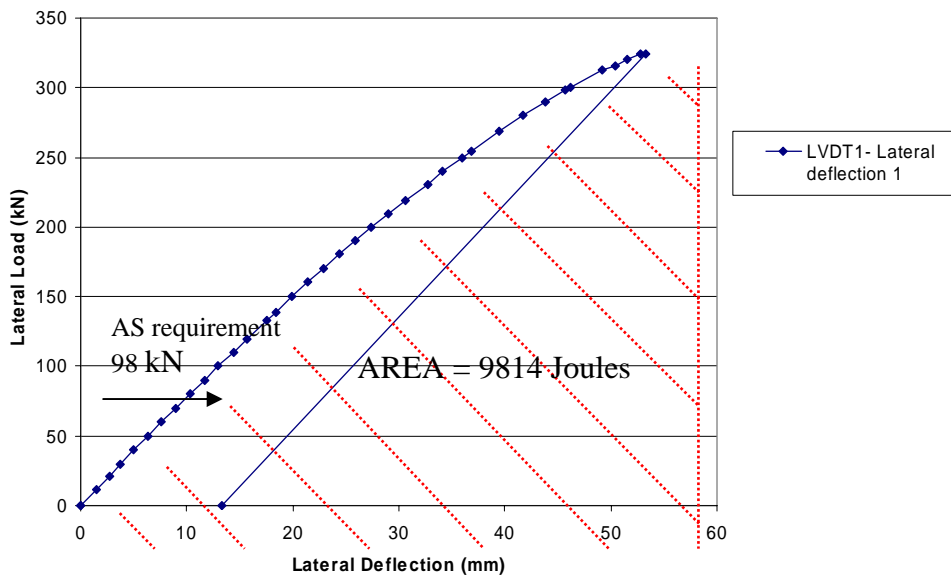


Figure 7 – Lateral load - deflection plot LVDT1

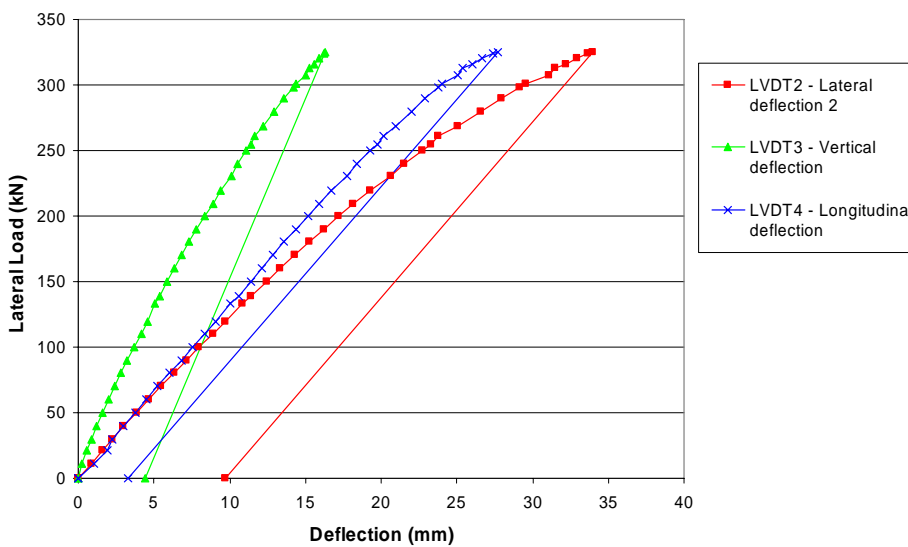


Figure 8 – Load- deflection plots: LVDT 2,3,4  
Vertical loading phase

A 150 tonne Enerpac hydraulic jack was used to deliver the required vertical load to the ROPS. The jack was mounted to a loading beam located directly above the ROPS and was positioned in line with the back face of the DLV. The load distribution device used for the vertical loading phase, employed the use of three steel reinforced bridge bearings that were sandwiched in between two 25mm thick plates. A ball and seat arrangement was similarly applied to the end of the jack and the combination of these two systems accounted for the predicted large forward and vertical deflection of the ROPS without damaging the jack. A stiff RHS loading beam was used to distribute the load evenly to each arm of the ROPS. An illustration of this load distribution device is presented in figure 9. The load was applied gradually and displacements and strains were recorded at regular intervals until the code specified load was achieved. Figure 10 shows the load deflection profile of the ROPS measured by each LVDT during loading, while figure 9 shows the deflected shape of the structure under the full vertical load. The 490 kN vertical load requirement was reached at a vertical deflection of 48mm. Once this load requirement was achieved the pressure in the jacks was released and resulted in approximately 14mm of permanent vertical deflection in the structure.



Figure 9 – ROPS under vertical load

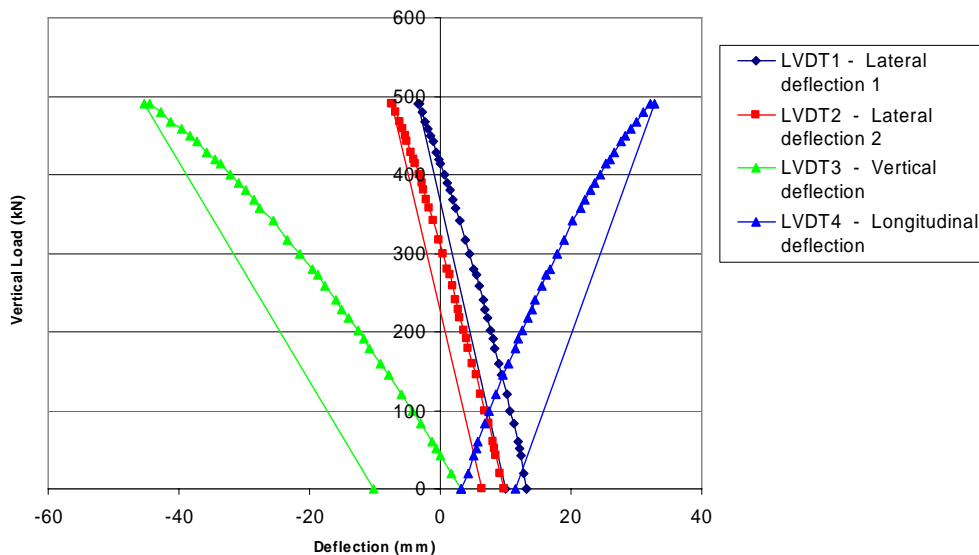


Figure 10 - Vertical load - deflection plots LVDT 1,2,3,4

#### Longitudinal loading phase

The final loading phase involved the application of the longitudinal load by means of an Enerpac 10t hydraulic jack. This jack was mounted to the loading frame and was positioned at the midpoint of the front horizontal cross member of the ROPS. The jack was accommodated with a ball and seat at each end to prevent damage during loading. Load spreading was permitted by employing a 50mm thick section of solid mild steel on the front face of the horizontal cross member of the ROPS. The load was gradually applied with the displacements and strains recorded at regular intervals until the code specified load was achieved. The deflected shape of the structure under the full longitudinal load can be seen in figure 11, while figure 12 displays the corresponding load deflection responses of the ROPS measured by each LVDT during the test. The 79 kN longitudinal load requirement was reached at a corresponding longitudinal deflection of 48mm. Unloading of the ROPS after the application of this load resulted in a net permanent longitudinal deflection of about 2 mm, which is effectively a reduction of 10 mm from the initial value of 12 mm.



Figure 11 - ROPS under Longitudinal load

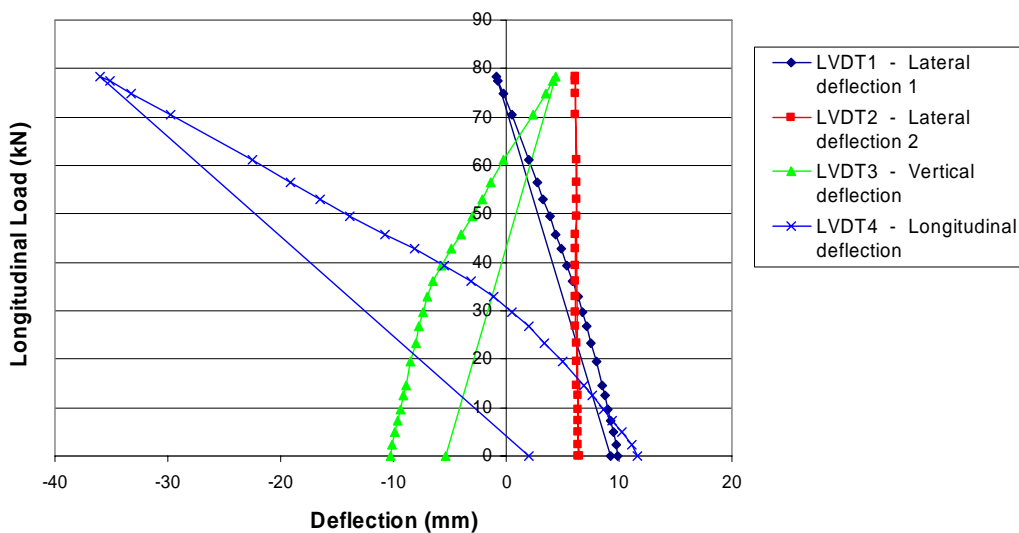


Figure 12 - Longitudinal load - deflection plots LVDT 1,2,3,4

### Finite element analysis of ROPS

A three dimensional finite element analysis of the ½ scale ROPS was conducted using the FEA package ABAQUS version 6.3. The geometry for the model was developed using the solid modeling package SOLIDWORKS to enable the inclusion of all corner radii for the RHS/SHS members of the ROPS. The established geometry was then imported into MSC PATRAN where the outer surface of the model was meshed using the S4R, four noded, large strain shell elements. A fine mesh density of 10mm was chosen for the model with some further refinement taking place in the corner radii regions. Figure 13 show graphically the FEA model for the ½ scale 630E ROPS.

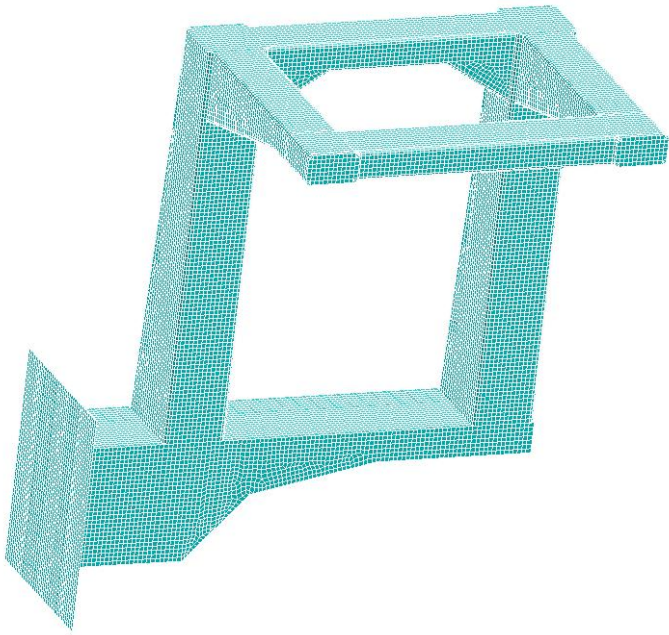


Figure 13 – FEA model

The FE model was subjected to a nonlinear finite element analysis that involved three loading stages which are outlined as follows:

- Lateral Loading and unloading
- Vertical loading and unloading
- Longitudinal loading and unloading

The nonlinear analysis procedure included the effects of large strains/displacements and utilized the automatic loading increment present within ABAQUS. Although the analysis was purely static and therefore did not include any inertia effects, unit load time histories were applied to each loading sequence. The maximum load values (amplitudes) and the durations of these load time histories, shown in figure 14, can be adjusted as required in the analysis. They were used to control the convergence of the solution and guide the structure gradually through each loading and unloading stage.

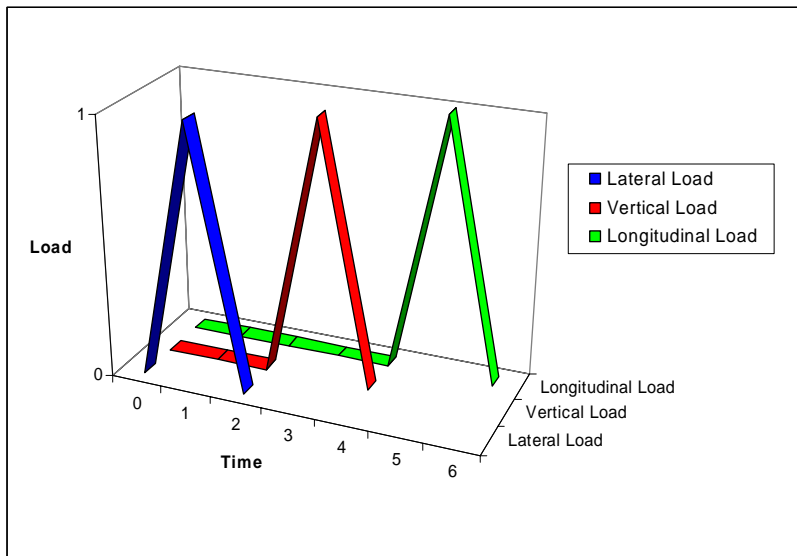


Figure 14 – Load time histories for FEA ROPS model

## FINITE ELEMENT MODEL

## Boundary conditions

In order to simulate the base fixity of the experimental model accurately, the FEA model of the ROPS was restrained about each translational degree of freedom, at twelve locations that corresponded to the position of the bolts that were used to connect the ROPS to the loading frame. Loading of the ROPS was achieved through the use of face pressures applied to the elements over a zone equivalent to that used in the experimental phase. In order to prevent excessive deformations in these regions, the thickness of the shell elements directly under the pressure loads was increased and given only elastic material properties. The pressure loads about each axis were combined into a single load case and the load time histories defined in figures 14 were used to guide the structure through each loading and unloading stage.

## Material Properties

The material properties used for the FE model were based on uniaxial tensile tests on specimens taken from the same RHS/SHS and the mild steel plate that was used to construct the ROPS and associated chassis beam. The material properties obtained from these tests, were then converted into true stress and plastic strain suitable for input into ABAQUS. Figure 15 show the engineering stress strain curve obtained from the testing of the specimens.

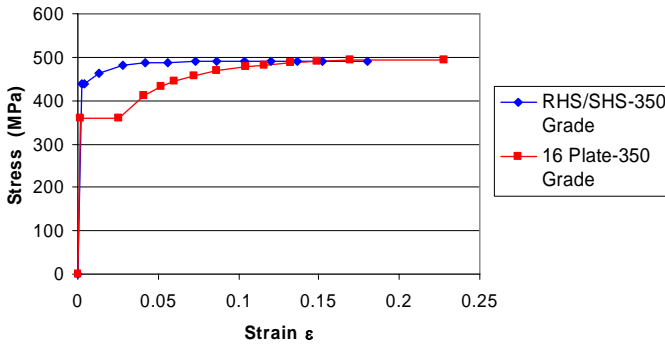


Figure 15 – ROPS material properties

## FEA Results

### Lateral Loading

Analysis of the ROPS under each loading stage resulted in the Von-Mises stress distributions presented in figures 17a, 19 and 20. The corresponding load deflection profiles for the lateral and vertical load cases are presented in figures 16 and 18. The load deflection plot under lateral load obtained from the finite element analyses (FEA) correlated extremely well with that obtained from the corresponding experimental phase.

Examination of the resulting Von-Mises stress distribution under the applied lateral load indicated significant yielding of the structure at the base of the left post as well as in the horizontal cross-member linking the two posts of the ROPS. This yielding can be verified by examination of figure 17 which shows red and orange stress contours within these regions respectively that corresponded to stress levels that had exceeded the yield stress of the ROPS material. Yielding of the ROPS in these zones was also verified by the strain rosette readings that were taken during the experimental lateral loading phase. Figure 17b shows the stresses at the base of the left post obtained from the strains recorded by rosette D.

During application of the vertical load, yielding took place along the length of each post, however, it was more pronounced and evenly distributed throughout the face of the left post only. The high stress distribution throughout each of these members is clearly highlighted by the orange stress contours that are displayed in figure 19. Examination of the resulting load deflection profiles obtained from FEA and the corresponding experimental phase indicated that the numerical model had a slightly stiffer response during this loading sequence. Both of these load deflection profiles have been plotted with reference to the structures pre-deformed position after removal of the lateral load.

The load deflection profile for the ROPS under the applied longitudinal load did not compare well with that obtained from the corresponding experimental loading phase. The FEA model predicted a fairly linear response with only small amounts of yielding taking place in localized regions, which had most likely resulted from the accumulated

stresses from the previous loading sequences. The reasons for these differences may also be attributed to the presence of residual stresses from heavy welding and the section geometry, that were not accounted for in the FEA model as well as the accuracy of the boundary conditions for the ROPS about this axis. Moreover, the longitudinal loading phase is the last phase in the loading sequence and the discrepancies between experimental and analytical results from the two previous phases (lateral and vertical) could accumulate to give a poor comparison for this particular phase. However, in real life, lateral impact is the most significant phase in which there is also an energy absorption criterion, and this will be the focus of the present research project. The calibrated FE model could be used with confidence to extend the investigation to the influence of parameters which enhance energy absorption and safety during lateral impact of the ROPS.

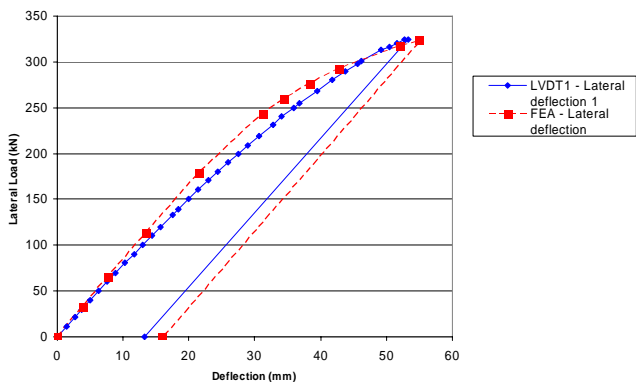


Figure 16 – Lateral load - deflection plot for FEA model

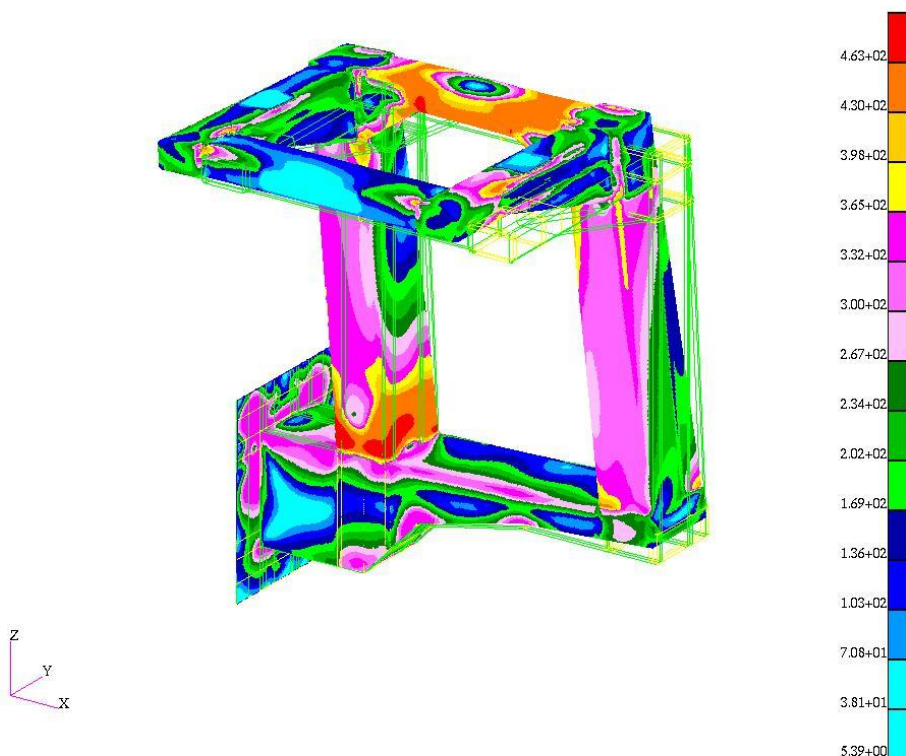


Figure 17a – Von-Mises stress distribution under lateral load

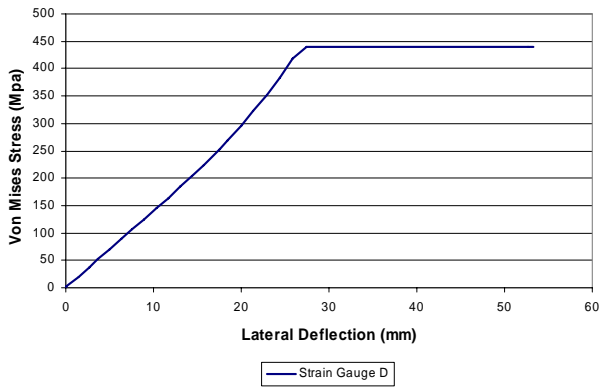


Figure 17b Stresses obtained from recording of strain gauge D - Von Mises Stress

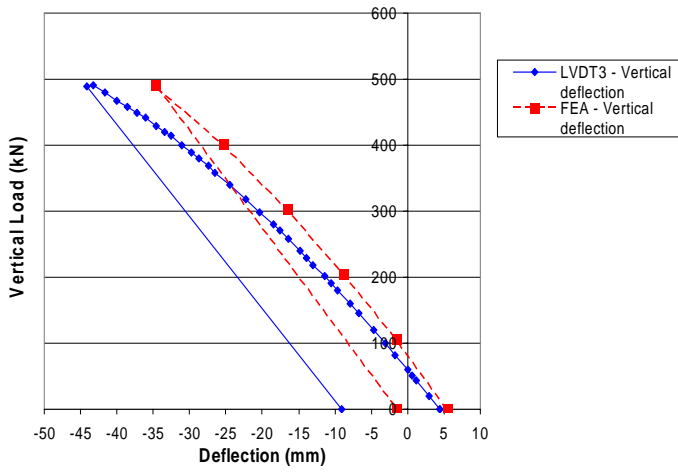


Figure 18 - Vertical load - deflection plot for FEA model

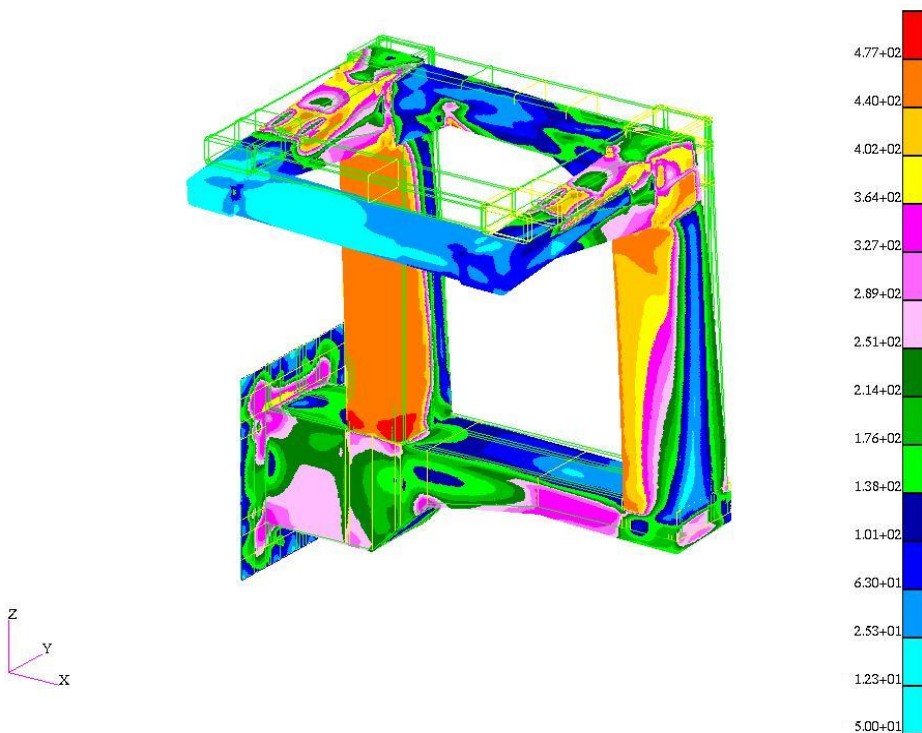


Figure 19 - Von-Mises stress distribution under vertical load

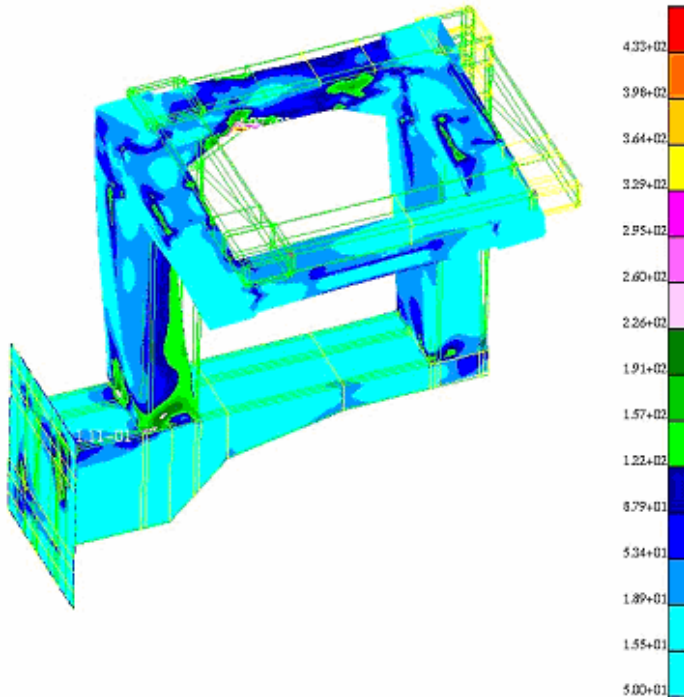


Figure 20 - Von-Mises stress distribution under longitudinal load

### Conclusion

An experimental investigation and a detailed finite element analysis of a rollover protective structure for a Dresser 630E dump truck at half scale was performed in accordance with current Australian standard performance criteria for ROPS. Comparison of the resulting experimental and FEA results indicated very good correlation under the lateral loading phase and good correlation under the vertical loading phase. The correlation of results under the longitudinal loading phase, which is the last phase and the least significant, was not good. The reasons for this could be attributed to the presence of residual stresses and cumulative errors from the previous loading phases, as mentioned earlier and inaccuracies in the modeling of the boundary conditions about this axis. Whilst some differences occurred between the experimental and FEA results, both indicated that the survival space known as the DLV, would not be impeded when subjected to loads in accordance with Australian and international ROPS standards. The proposed analytical modeling technique employs unit load time histories, a convenient feature available in the finite element program, to guide the ROPS through each loading and unloading stage and was found to be a successful method for analysing ROPS, under the lateral and vertical loading phases. Further study will look at increasing the level of energy absorption for the ROPS by incorporating supplementary energy absorbing devices as well as a more appropriate stiffness distribution for the ROPS. In addition to this, the present study has demonstrated that it may be feasible to use calibrated finite element models to carry out dynamic simulations to verify the adequacy of current standard procedures, and in optimizing the energy absorption during the lateral loading phase to enhance the level of safety provided to the occupants of heavy vehicles.

### References

AS 2294.2-1997 Australian Standard Earth-moving machinery-Protective Structures: Part 2: Laboratory tests and performance requirements for rollover protective structures

Clark, B.J., Thambiratnam, D.P., Perera, N.J., Barker, N., Behaviour of Rollover Protective Structures - An Experimental Study, Proceedings, 3rd European Conference on Steel Structures, Coimbra, Portugal, 2002.

Hunckler C.J., Purdy R.J., and Austin R.D., Non-linear Analysis of the Terex Scraper Rollover Protective Cab, Proc Earthmoving Industry Conf. – Society of Auto-motive Engineers, Peoria, IL USA., 1985.

Kim T.H., Reid S.R., Multiaxial softening hinge model for tubular vehicle rollover protective structures, *Mechanical Sciences*, 2001, 43: 2147-2170

Srivastava, A.K., Rehkugler, G. E., Masemore, B.J., Similitude Modelling Applied to ROPS Testing, *Transaction of the ASAE*, Vol 21, Issue 4, July-August 1978, pp 633-645.

Swan, S.A. (1988), Rollover Protective Structure Performance Criteria for Large Mobile Mining Equipment, United States, Bureau of Mines n9209 1988 20p Bureau of Mines, Mineapolis, MN, USA.

Tomas J.A., Sheffield S.R., Altamore P.F., Computer Simulation of ROPS for Earthmoving Vehicles, *Quarry Magazine*, 1997